

**EVALUATING UNMANNED AERIAL VEHICLE BASED CROP INDEXING
TECHNIQUES: MODIFIED CONSUMER GRADE RGB VS. MULTISPECTRAL**

by

CHRISTOPHER F. SOLECKI

A THESIS SUBMITTED IN PARTIAL FULFILLMENT
OF THE REQUIREMENTS FOR THE DEGREE OF
BACHELOR OF NATURAL RESOURCE SCIENCE (HONS.)

IN THE DEPARTMENT
OF
NATURAL RESOURCE SCIENCES
AT
THOMPSON RIVERS UNIVERSITY

THESIS EXAMINING COMMITTEE

John S. Church (Ph.D.), Thesis Supervisor & Associate Professor,
Dept. Natural Resource Sciences

David J. Hill (Ph.D.), Associate Professor, Dept. Geography and Environmental Studies

Garrett Whitworth (Ph.D.), Post-Doctoral Fellow, Faculty of Science

Lauchlan Fraser (Ph. D), Professor, Dept. Biological Sciences

Dated the 12th day of May 2017, in Kamloops, British Columbia, Canada

Abstract

Thesis Supervisor: Associate Professor John S. Church

The use of unmanned aerial vehicles (UAVs) in agriculture is a relatively new and rapidly expanding concept. By using UAVs equipped with multispectral near infrared sensors, farmers and land managers can detect intra-field crop variability which enables adjustments to be made to crop applications and other management decisions. This type of management has been termed precision agriculture and employs the use of various crop indices such as the normalized difference vegetation index (NDVI). The NDVI is one of the most common crop indices; and is used to measure relative chlorophyll content in green vegetation. In this study, I investigated the sensing abilities of two aerial cameras to determine whether filter modified consumer cameras can produce NDVI maps equivalent to those produced by a multispectral camera. I compared a MicaSense RedEdge[®] multispectral camera to a modified DJI Zenmuse X3 camera, mounted simultaneously onboard a DJI Inspire 1 UAV, with respect to their ability to generate reliable NDVI maps using Pix4D photogrammetry software. Through evaluation of the index maps produced by the two cameras, the MicaSense RedEdge[®] was found to produce index values that were more representative of the study site than the modified DJI Zenmuse X3. Spatial vegetation patterns observed by the two sensors were also determined to be significantly different. This study revealed that the two sensors did not produce equivalent NDVI results, and multispectral cameras appear to be a more accurate tool for examining crop productivity and variability.

Table of Contents

Abstract	i
List of Figures	iii
List of Tables:	iv
Acknowledgements:	iv
Introduction	1
Materials and Methods	5
Image Acquisition and Processing.....	5
Statistical Analysis	8
Results	9
Index Values	9
Spatial Variations.....	12
Discussion	14
Processing Images.....	14
Index Values	15
Spatial Variation	17
Image Format	17
Conclusions	18
Literature Cited	19
Appendix A.....	22
Appendix B.....	26
Appendix C.....	30
Appendix D	31

List of Figures

Figure 1: Transmission curve for the modified DJI Zenmuse X3 camera following modification with the band pass filter. Only red (660 nm) and near infrared (850 nm) wavelengths of light can pass through the filter to the sensor (adapted from [Aerial Media Pros 2015]).....	3
Figure 2: Transmission curve for the MicaSense RedEdge® multi-spectral camera. Blue (475 nm), green (560 nm), red (668 nm), red edge (717 nm), and near infrared (840 nm) are captured by the sensor (Adapted from [MicaSense 2016]).	4
Figure 3: DJI Inspire 1 quadcopter with modified Zenmuse X3 and MicaSense RedEdge® simultaneously mounted.	6
Figure 4: Example of NDVI maps produced by pix4D photogrammetry software. Shown are NDVI maps from August 23rd from the MicaSense RedEdge® (left) and the modified X3 (right). Green represents areas with high relative NDVI values while red represents areas with low relative NDVI values.	10
Figure 5: Mean NDVI values for NDVI orthomosaics for the four sampling dates. Error bars represent +/- 1 S.D.	11
Figure 6: Example of NDVI maps once they had been separated in 20% quantiles and assigned ordinal ratings of 1 to 5. Maps shown are from the August 23rd sampling date from the MicaSense RedEdge® (left) and the modified X3 (right).	13
Figure 7: NDVI orthomosaics from the MicaSense RedEdge® (left) and the modified DJI X3 (right) for July 11 th , 2016.....	22
Figure 8: NDVI orthomosaics from the MicaSense RedEdge® (left) and the modified DJI X3 (right) for July 13 th , 2016.....	23
Figure 9: NDVI orthomosaics from the MicaSense RedEdge® (left) and the modified DJI X3 (right) for August 19 th , 2016	24
Figure 10: NDVI orthomosaics from the MicaSense RedEdge® (left) and the modified DJI X3 (right) for August 23 rd , 2016	25
Figure 11: NDVI maps once they had been separated in 20% quantiles for the July 11 th , 2016 sampling date from the MicaSense RedEdge® (left) and the modified DJI X3 (right).....	26
Figure 12: NDVI maps once they had been separated in 20% quantiles for the July 13 th , 2016 sampling date from the MicaSense RedEdge® (left) and the modified DJI X3 (right).....	27
Figure 13: NDVI maps once they had been separated in 20% quantiles for the August 19 th , 2016 sampling date from the MicaSense RedEdge® (left) and the modified DJI X3 (right).....	28
Figure 14: NDVI maps once they had been separated in 20% quantiles for the August 23 rd , 2016 sampling date from the MicaSense RedEdge® (left) and the modified DJI X3 (right).....	29
Figure 16: The DJI Zenmuse X3. This camera has a single lens and one 12 mega-pixel sensor with a Bayer filter array.	31
Figure 17: The MicaSense RedEdge® multispectral camera. This camera has 5 lenses, one for each spectral band, and 5, 1.2 mega-pixel sensor chips with a separate filter for each chip.	31

List of Tables:

Table 1: Minimum, maximum, standard deviation and mean NDVI values for the MicaSense RedEdge® and modified X3 NDVI maps for July 11 th , July 13 th , August 19 th , and August 23 rd ..	9
Table 2: Results of the Wilcoxon Signed Ranks test showing the standardized test statistic and the significance of the test.....	30

Acknowledgements:

I would like to thank my thesis supervisor John Church for providing me with the project idea as well as all the equipment that was needed to collect the data. Thank you John for including me on the drone team, and for allowing me to be involved in various projects over the past couple of years. I really appreciate all the help you have given me. I would also like to thank the rest of my committee members. Thanks to David Hill for providing me with some guidance in finding a way to compare these two cameras. Doing so would have been a lot harder without your insight. Thank you, Garrett, for providing input and suggestions into my project along the way and for sharing the MicaSense with me over the summertime. Thank you Lauch for your feedback on the project that helped me add some extra strength to my statistics.

Introduction

The use of unmanned aerial vehicles (UAVs) in agricultural management is a relatively new and rapidly advancing field (Van der Meij 2016). Declining costs and increasing capabilities of consumer-grade UAVs have made them more useful, convenient, and accessible to consumers and farmers alike. UAVs provide an advantage over traditional methods of acquiring remote sensing data (helicopters, fixed wing aircraft, and satellites) in that operational costs are lower, they have more flexibility, and spatial resolutions are greater (Matese et al. 2015). The integration of UAVs into agricultural management has become increasingly popular with the emergence of what is termed Precision Agriculture (PA), which uses technology to increase management precision and efficiency by strategically placing crop additives, such as pesticides and fertilizer, in order to reduce inputs while maximizing outputs (Candiago et al. 2015). This type of management strategy uses ground sensing techniques such as multi-spectral imaging to evaluate plant productivity and vigor, which is typically done through the generation of vegetation indices (Candiago et al. 2015).

Vegetation indices are a way of using the reflectance of different wavelengths of incident light to give us information about the characteristics of vegetation (Herring 2000). The normalized difference vegetation index (NDVI) is one of the most commonly used indices and looks specifically at the red (620 - 780 nm) and near infrared (NIR)(800 - 2500 nm) regions of the electromagnetic spectrum (Herring 2000). This index is useful for determining the productivity of vegetation because (1) chlorophyll absorbs light strongly in the red region of the spectrum while leaf cell structure reflects strongly in the NIR region (Monteith 1972); and (2) the rate of photosynthesis is positively correlated with the amount of photosynthetically active radiation absorbed by the plant (Pavlović et al. 2014). This assumes that a higher rate of photosynthesis is indicative of higher chlorophyll concentrations as well as productive vegetation; therefore, more chlorophyll indicates greater plant productivity (Pavlović et al. 2014). Capturing reflectance data overtop of crops

can therefore allow us to derive measures of crop productivity using NDVI and similar indices.

Multi rotor UAVs offer an affordable and user friendly platform to mount airborne sensors on to capture images of crops. Typically, an automated grid pattern is flown over top of the target area with images being captured at predetermined intervals with a set overlap and height. Once images of a crop have been captured, processed into an orthomosaic and an index map is created, the information contained in the index map can be quantified into different regions for application. By examination of the NDVI and other similar indices (such as the green normalized difference vegetation index and the soil adjusted vegetation index) managers are able to identify variability within crops; and make adjustments to applications rates of crop additives such as fertilizer and pesticides by employing variable rates of application (Candiago et al. 2015; Matese et al. 2015). The ability to detect and account for intra-field variability, and employ variable rate spreading instead of uniform application over the entire crop, has the potential to save costs on crop additives, lower environmental costs induced by leeching of excess nutrients and chemicals, and increase crop yields (Matese et al. 2015).

Modified cameras, such as the modified DJI Zenmuse X3 (Appendix D, Figure 15) used in this study, refer to standard consumer digital cameras (capturing red, green, and blue bands of light; RGB) that have been modified by altering the filter configuration (Taylor 2015). The modified camera used in this study has had the infrared blocking filter removed, and a lens with a band pass filter added which allows only red and near infrared wavelengths to pass through the lens at 25 nm band widths for each band. This modification allows near infrared light to pass through as well as the red band so that NDVI can be calculated (Aerial Media Pros 2015). The Zenmuse X3 camera has a 12 megapixel complimentary-metal-oxide-semiconductor (CMOS) sensor with a Bayer filter array (DJI 2017). Once the new filter is installed, the camera effectively has two filters: the band pass filter and the Bayer filter array which is situated directly on top of the sensor. The transmission curve for this cameras lens is shown in Figure 1. This transmission curve shows

the specific bands of light that are able to pass through the filter band pass filter, however, it does not show the transmission of the micro-filters on the Bayer filter array.

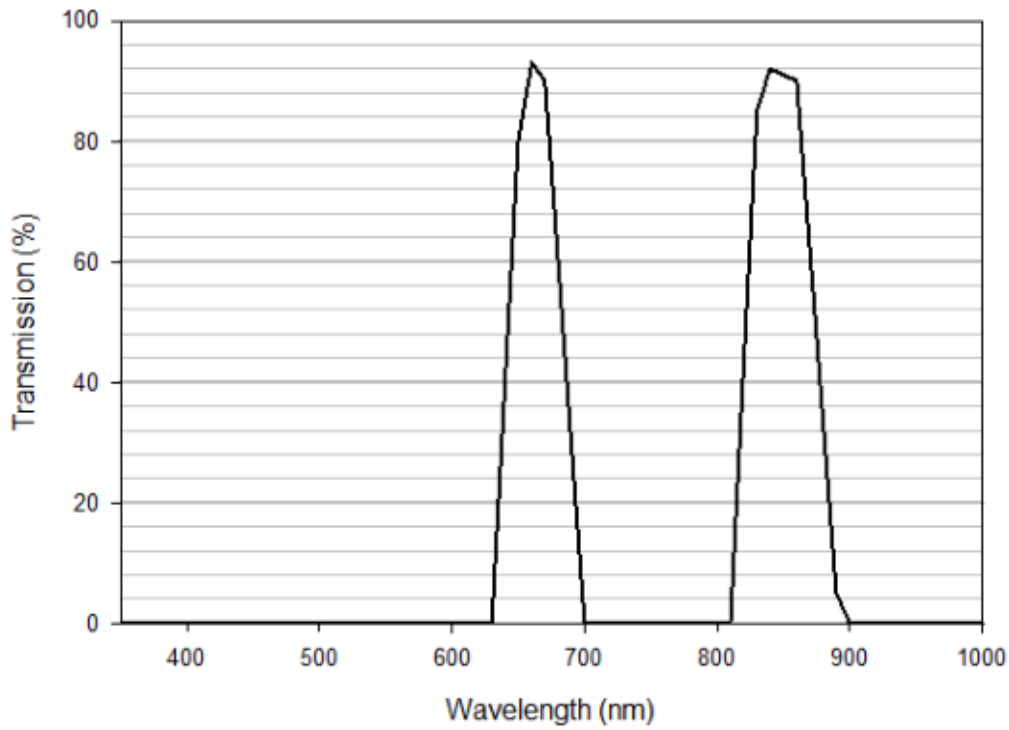


Figure 1: Transmission curve for the modified DJI Zenmuse X3 camera following modification with the band pass filter. Only red (660 nm) and near infrared (850 nm) wavelengths of light can pass through the filter to the sensor (adapted from [Aerial Media Pros 2015]).

Multi-spectral cameras like the MicaSense RedEdge® (5-band)(Appendix D, Figure 16) simultaneously capture discrete bands of light through separate lenses (MicaSense 2016). The MicaSense RedEdge® captures 5 bands of light in the blue (475nm), green (560 nm), red (668 nm), red edge (717 nm), and near infrared (840 nm) regions of the spectrum (Figure 2). This camera has a 1.2 megapixel CMOS sensor for each of the five bands that it captures (2017 personal communication with MicaSense support).

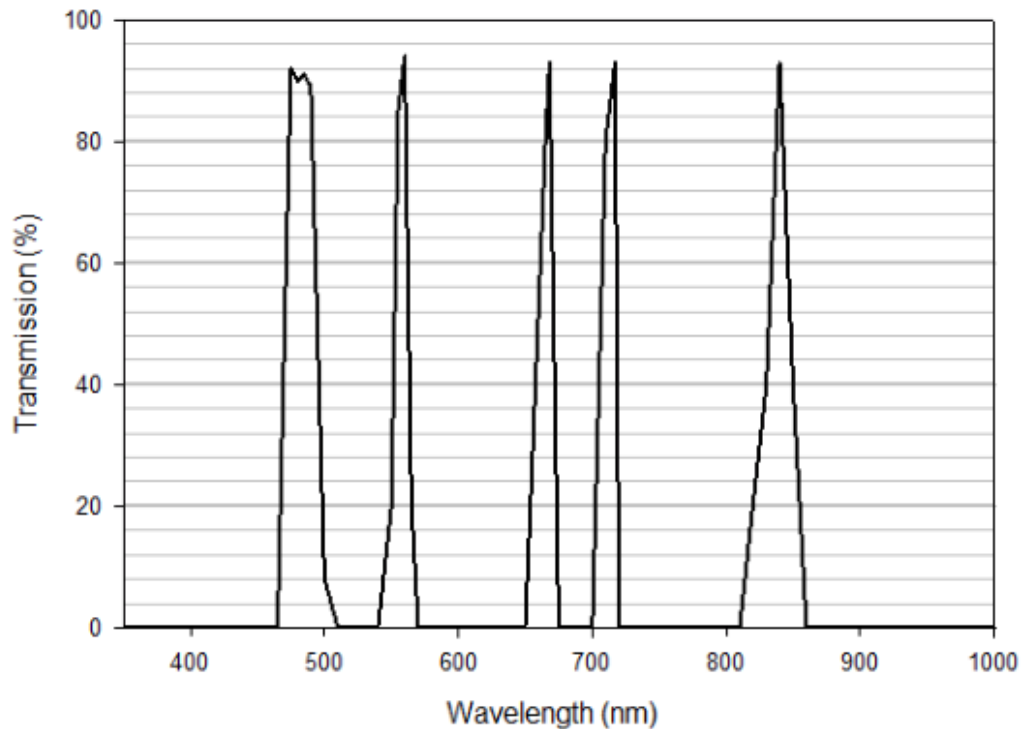


Figure 2: Transmission curve for the MicaSense RedEdge® multi-spectral camera. Blue (475 nm), green (560 nm), red (668 nm), red edge (717 nm), and near infrared (840 nm) are captured by the sensor (Adapted from [MicaSense 2016]).

The proposed advantage of modified cameras is that they offer similar results to multi-spectral cameras at a much lower cost; and essentially any digital camera could be turned into a tool for precision agriculture by simply removing the infrared blocking filter. An Aerial Media Pros modified DJI Zenmuse X3 retails for \$1740.66 CAD (Aerial Media Pros 2015), while the MicaSense RedEdge® multispectral camera retails for \$7906.00 CAD (MicaSense 2016). While modified cameras may offer a lower cost of data collection in terms of initial capital acquisition, the reliability of data acquired from these cameras has not been well demonstrated in the literature (Lebourgeois et al. 2008; Klaas 2016).

Matese et al. (2015) present evidence that the UAV platform is most useful on smaller scales (5 ha or less) as they provide greater resolutions, and thus are more capable of detecting variability within crops with high levels of heterogeneity. While comparisons between various sensing platforms (UAV, aircraft, and satellite) have been conducted (Nex and Remondino 2014; Matese et al. 2015), and have identified UAV's as a cost-effective

method of data acquisition, there is debate over whether low cost, modified consumer grade RGB cameras can offer reliable NDVI results as compared to NDVI produced by multi-spectral cameras. Previous work has found varying results when analyzing crop indices from modified cameras with some supporting their use (Lebourgeois et al. 2008), and some finding spectral contamination in modified cameras significantly reduces accuracy (Klaas 2016).

For this study, I examined the NDVI maps that were produced by the MicaSense RedEdge® 5-band multi-spectral camera and compared it to a modified DJI Zenmuse X3 to determine whether the modified X3 camera will provide a similar output with respect to NDVI values, and the spatial patterns in vegetation productivity that are recognized by the sensor. My null hypotheses are that (1) the modified camera will produce NDVI index maps that are equivalent (not statistically different) to those produced from the MicaSense RedEdge®, and (2) the same spatial variations in vegetation will be recognized by both cameras.

The objectives for my study were to:

- simultaneously capture images with both cameras overtop of the plot area;
- generate normalized difference vegetation indices (NDVI) from the images obtained by both cameras
- determine whether NDVI values differ between camera;
- determine whether the same spatial variation in vegetation is recognized by both cameras

Materials and Methods

Image Acquisition and Processing

All images acquired from the cameras were taken over top of a square 250x250m grass forage plot located at Tatalrose Ranch inc. in Grassy Plains, British Columbia. The plot

was seeded with a forage mix of 21% smooth brome (*Bromus inermis*), 9% orchard grass (*Dactylis glomerata*), 2% timothy (*Phleum pretense*), 29% 4-star alfalfa (*Medicago sativa*), 32% red clover (*Trifolium pratense*), and 7% yellow blossom alfalfa (*Medicago falcata*). The approximate location of the plot is 53°58'55.69"N, 125°58'42.66"W. Both cameras were mounted simultaneously on the DJI Inspire 1 quad-copter for all flights. The modified X3 was mounted on the aircrafts factory gimbal and the MicaSense RedEdge® was attached using a custom mounting plate securing it to the back of the aircraft (Figure 3). Grid flight patterns overtop of the plot were generated using the Pix4D mapper capture application and were flown at a height of 40 m. Images captured by the modified X3 were saved by default in 8-bit JPEG format while the images captured by the RedEdge® were stored as 16-bit RAW Tiff files. The X3 was powered by the battery on the UAV, while the RedEdge® was independently powered by a GoPro battery.



Figure 3: DJI Inspire 1 quadcopter with modified Zenmuse X3 and MicaSense RedEdge® simultaneously mounted.

Prior to initiation of all flights, weather conditions were recorded including wind speed, temperature, and cloud cover. Time since last precipitation, time of flight, and the average maturity of the crop were also recorded. Immediately prior to the first flight on each day, images of a spectralon calibration target were taken to calibrate images to the degree of incoming solar radiation. As cloud cover was generally high, and persisted for the majority of the field season, I attempted to select days with similar cloud conditions (based

on visual observation) in order to keep variability of incoming solar radiation low. Flights consisted of 4 – 150 x 150 m grid flights at 40 meters above ground level, resulting in a 300 x 300 m square area being covered. 300 x 300 m was used to ensure that the entire plot area (250x250 meters) was encompassed by the flight. All flights were initiated between 12:00 pm and 1:00 pm local time, and flights were completed within 1 to 1 ¼ hours of the start time.

Images were then processed to produce orthomosaics using Pix4D photogrammetry software. Images were calibrated using the images of the spectralon calibration target and the Pix4D camera calibration tool. Once step 1 of processing in Pix4D had been completed, five 3-dimensional ground control points (GCPs) were added to each map (each GCP was marked on a minimum of two images) to increase the positional accuracy of the maps. Pix4D is a software package that allows users to take georeferenced images captured with a UAV or aircraft, and stitch these images together into orthomosaics, digital surface models, terrain models, and point clouds (Pix4D 2017a). The software is meant to allow consumer level UAVs to be used as mapping and surveying tools (Pix4D 2017a).

The orthomosaics created in Pix4D were used to generate a reflectance map from which the NDVI map was obtained. The NDVI formula that was used in the Pix4D raster calculator for the MicaSense RedEdge® is as follows:

$$NDVI = \frac{\rho_{nir} - \rho_{red}}{\rho_{nir} + \rho_{red}}$$

Where NDVI is the normalized difference vegetation index, ρ_{nir} is the near infrared band, and ρ_{red} is the red band.

The formula used in the raster calculator for the modified Zenmuse X3 camera was slightly different, as the camera captures the reflectance data from the near infrared band in the location that the standard, unmodified camera captures reflectance data for the blue band and is as follows:

$$NDVI = \frac{\rho_{blue} - \rho_{red}}{\rho_{blue} + \rho_{red}}$$

Where NDVI is the normalized difference vegetation index, ρ_{blue} is the band storing information for the near infrared band, and ρ_{red} is the red band.

Statistical Analysis

In order to test for significant differences in NDVI values between the two cameras and between the four sampling dates, a two-way ANOVA ($\alpha=0.05$) was done using IBM SPSS statistical software (IBM Corp. 2016). Prior to the two-way ANOVA, each of the groups of the two independent variables were tested for normality and homogeneity of variance using SPSS (IBM Corp. 2016). Camera and date were used as the two factors for the test; and 1100 sample pixels were randomly selected from each of the index maps using ArcMap software (ESRI 2016).

To determine whether the two sensors were recognizing the same spatial patterns in the vegetation across the plot, further processing of the orthomosaics was needed. A GeoTiff of each index map was exported from Pix4D software and loaded into an R-Studio working directory (R Core Team 2016). The GeoTiff files contained coordinates and an NDVI value for each pixel. To statistically compare each set of NDVI maps the index values from each map were separated into quantiles of 20 percent for a total of five categories. Once the quantiles were created, ordinal values from 1 to 5 were assigned to each category of values with five representing the highest NDVI values and 1 representing the lowest NDVI values (e.g. if an NDVI value was 0.92 and 20% of all the index values for the map were above 0.90, then it would be designated as a five). The transformed index maps were then exported from R-Studio as a GeoTiff.

GeoTiffs were then imported into ArcMap GIS software (ESRI 2016). Using the pixel inspector tool and the X,Y coordinate locator, random samples were collected from each of the modified X3 index maps. A sample from the same coordinates were then taken from the corresponding MicaSense RedEdge® index maps for each date. Sample coordinates were selected using a random number generator to produce a latitude and longitude within the map extent. A total of 5, 220 pixel samples were drawn from each map for a total of 1,100

pixel values. SPSS statistical software was used to compare paired samples from each map using a Wilcoxon matched pairs signed ranks test ($\alpha=0.05$).

Results

Index Values

Table 1 displays the minimum and maximum values as well as the mean value for the entire raster obtained from each of the NDVI maps generated from the modified DJI X3 and the MicaSense RedEdge® images. An example of the NDVI maps produced by Pix4D for both of the cameras can be seen in (Figure 4). Green indicates areas that have higher NDVI values while red indicates low NDVI values. The NDVI maps for both cameras for all four sampling dates can be found in Appendix A. The mean NDVI values were higher for the MicaSense RedEdge® for all index maps and all values obtained from the modified X3 were negative. Mean values from the MicaSense RedEdge® decreased with each successive sampling period but this trend was not present for the modified X3. Standard deviations for index maps from the MicaSense RedEdge® were also larger.

Table 1: Minimum, maximum, standard deviation and mean NDVI values for the MicaSense RedEdge® and modified X3 NDVI maps for July 11th, July 13th, August 19th, and August 23rd.

	X3				RedEdge®			
	Mean	Min	Max	Std. Dev.	Mean	Min	Max	Std. Dev.
July 11 th	-0.164	-0.60	-0.16	0.0151	0.901	0.67	0.96	0.0232
July 13 th	-0.174	-0.54	-0.04	0.0195	0.901	0.67	0.90	0.0199
Aug. 19 th	-0.136	-0.98	-0.01	0.0236	0.589	0.24	0.87	0.0778
Aug. 23 rd	-0.149	-0.98	-0.02	0.0420	0.366	0.00	0.76	0.0994

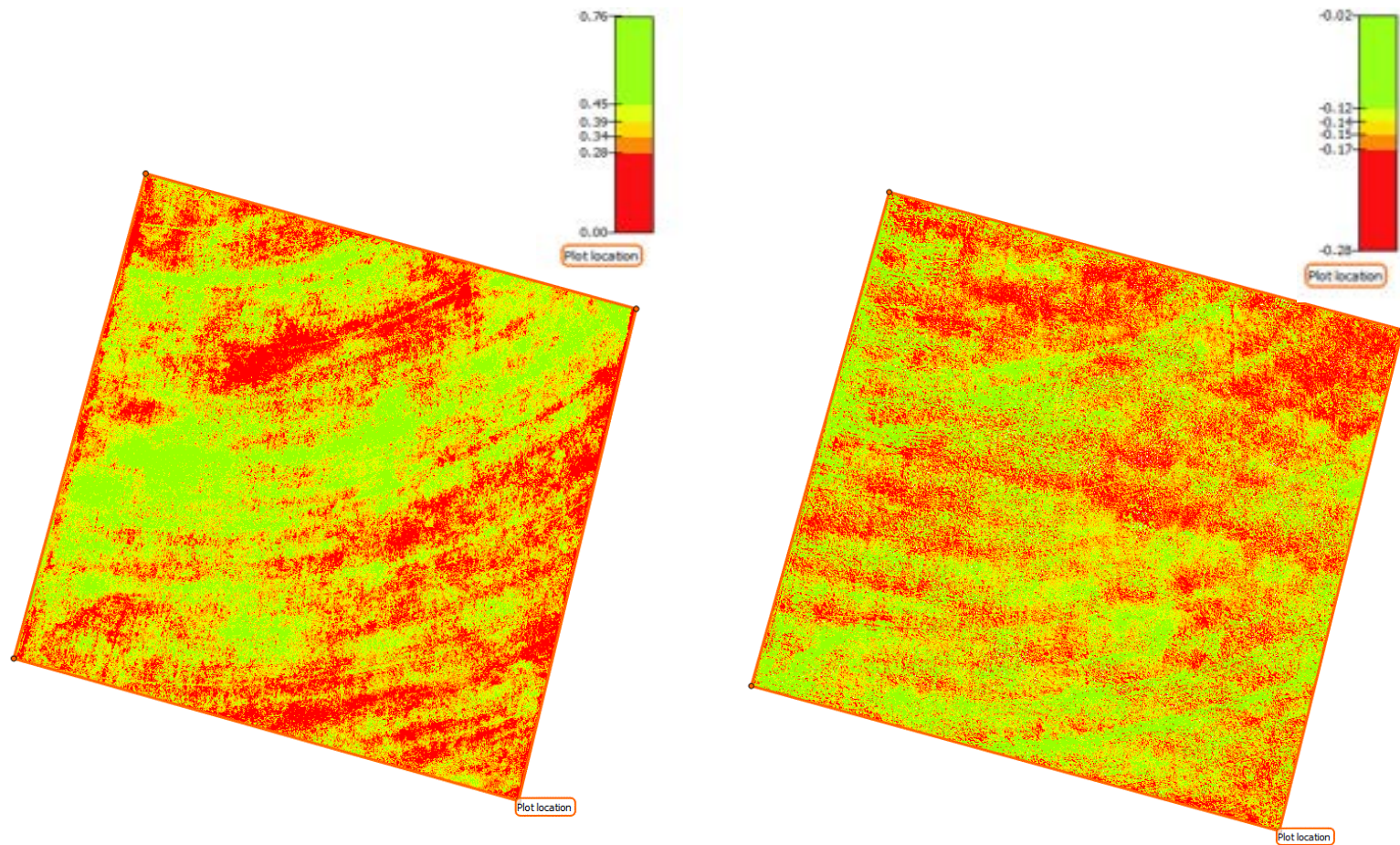


Figure 4: Example of NDVI maps produced by pix4D photogrammetry software. Shown are NDVI maps from August 23rd from the MicaSense RedEdge® (left) and the modified X3 (right). Green represents areas with high relative NDVI values while red represents areas with low relative NDVI values.

Figure 5 shows mean NDVI values from Table 1 plotted over time. NDVI value was significantly related to the camera model that captured the images ($P < 0.0001$), and NDVI values for the MicaSense RedEdge[®] were higher than the X3 for all dates. NDVI value was also significantly related to the date that the image was captured on ($P < 0.0001$), and NDVI values for the MicaSense RedEdge[®] declined as date progressed. There was also a significant interaction between camera and date. Index value by date was significantly related to camera model that captured the images ($P < 0.0001$).

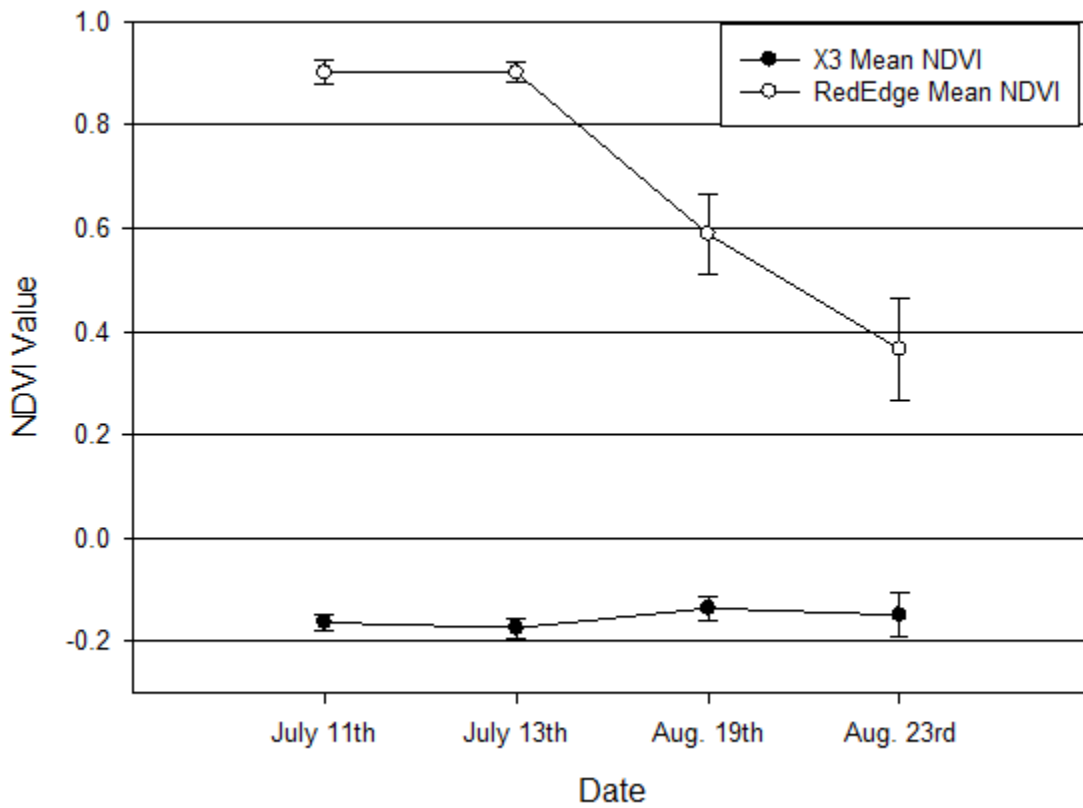


Figure 5: Mean NDVI values for NDVI orthomosaics for the four sampling dates. Error bars represent +/- 1 S.D.

Spatial Variations

Figure 6 shows an example of the NDVI index maps once they had been separated into 20% quantiles and assigned values from 1 to 5. The scale bar in the upper right corner shows the ordinal rating scale and black and white color palette where a 1 (white) represents areas of low relative NDVI values while 5 (black) represents areas of high relative NDVI values. The spatial patterns that were recognized by the MicaSense RedEdge® were significantly different ($P < 0.0001$) for all dates except for July 13th ($P = 0.08$). A summary of results from the Wilcoxon signed ranks test between the two cameras on each date can be found in Appendix C, Table 2.

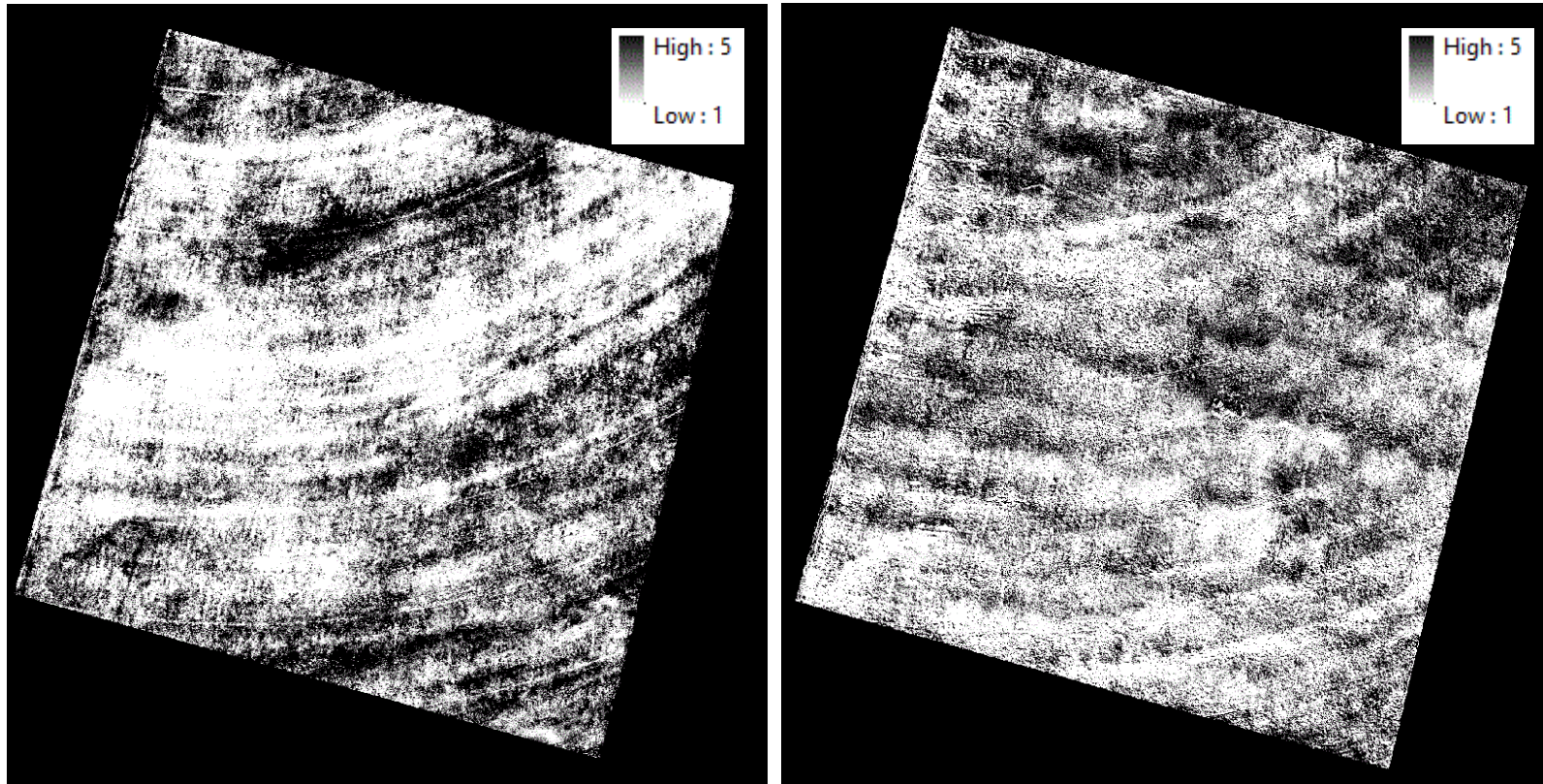


Figure 6: Example of NDVI maps once they had been separated in 20% quantiles and assigned ordinal ratings of 1 to 5. Maps shown are from the August 23rd sampling date from the MicaSense RedEdge® (left) and the modified X3 (right).

Discussion

In this study, I looked at the differences in NDVI maps produced by two different cameras to assess whether they are producing similar NDVI values. Multi-spectral imagers have been looked at before in comparison with modified consumer cameras, and have been proven to produce values that are close to that of a field spectrometer (assuming the same filter configuration), which is regarded as the most accurate way to measure reflectance in the field (Nebiker et al. 2016). Previous studies have found mixed results when examining modified consumer cameras, with some finding modified cameras very similar to multispectral cameras with respect to quantitative and qualitative measurements (Lebourgeois et al. 2008); and some finding that only qualitative analysis is possible from these cameras (values are different than field spectrometer measurements but patterns are still recognized correctly) (Klaas 2016; Nebiker et al. 2016).

In summary, the main results from this study were as follows:

- NDVI maps produced by the MicaSense RedEdge® and modified X3 camera did not display similar index values. The MicaSense produced positive values while the modified X3 produced negative values;
- NDVI values were significantly correlated with the camera that captured the images;
- The two cameras did not recognize the same spatial variation in NDVI values.

Processing Images

The MicaSense RedEdge® had greater ease of processing than the modified X3 camera. Data processing for the modified X3 was more difficult as the Pix4D photogrammetry software produced more errors in processing of the images obtained by this camera which resulted in issues with stitching images together. The issue may be that the program recognized the modified camera as an unmodified Zenmuse X3. As the modified camera has a different lens and filter configuration than the factory model, adjustments to camera parameters in the pre-processing stage had to be made (2016 email

from Pix4D support). The quality report that summarizes Pix4D processing of orthomosaics identified high relative differences between optimized and internal camera parameters for the modified X3. The modified X3 had an average of 16.87% difference between initial and optimized camera parameters, even once the recommended adjustments to camera settings were made. In comparison, the MicaSense RedEdge® had an average of only 0.32%. This may be a reason for processing errors experienced with the Modified X3 (Pix4D 2017b).

From visual observations of the index maps it appeared that the modified X3 camera was impacted largely by vignetting effects. Vignetting refers to the reduction in sensor saturation as you move farther away from the center of an image; meaning that as you get closer to the edges of the photo, digital numbers (DN)(a variable value that is assigned to each pixel) will decrease, and the image darkens (Pix4D Support 2016). Pix4D software automatically corrects for vignetting effects when generating the reflectance maps (Pix4D Support 2016), however it appeared that effects from vignetting were still prevalent following processing; and this likely had an impact on generation of index maps as well as NDVI values (Lebourgeois et al. 2008).

Index Values

NDVI values from the MicaSense RedEdge® camera followed a logical trend as time progressed throughout the field season (Table 1 and Figure 5). Following seed production and maturation of grass, chlorophyll concentrations begin to decrease and dry matter content within the plant increases (Cordon et al. 2016). It was noted on August 12th that the grass crop had reached full maturity and had begun to senesce. As the chlorophyll concentrations decline, we should see a subsequent decline in NDVI values. The MicaSense RedEdge® NDVI values decreased from the July 11th flight onward which is logical, however the modified X3 NDVI values did not follow this trend. Based on this information the RedEdge® appears to be more effective at recognizing chlorophyll concentrations based on NDVI.

Negative NDVI values are characteristic of areas with no vegetation such as bare soil or rock, at least when the true reflectance is captured (Candiago et al. 2015). The modified

DJI X3 (modified X3) produced all negative values for all index maps while the MicaSense RedEdge® produced all positive values (Table 1 and Figures 7, 8, 9, and 10). The proximal cause of the negative values produced by the modified X3 is the low level of near infrared light that is being registered by the sensor relative to red light. In green vegetation, there should be more near infrared light reflected than red light and NDVI values are expected to be above 0 (Herring 2000).

Low relative levels of near infrared light could occur for more than one reason. Lebourgeois et al. (2008) attributed low DN's of near infrared light to underexposure of the images resulting in low values in the near infrared region. A more likely cause however is that the overlapping of spectral channels in modified cameras can cause near infrared values to be lower than expected relative to other wavelengths, which has been documented in other studies (Verhoeven et al. 2009; Nebiker et al. 2016). Spectral overlap occurs because the infrared blocking filter has been removed, and because silicon sensors are very sensitive in the near infrared region of the spectrum (Darmont 2009), it allows the photodiodes of the sensor to absorb photons in the near infrared region. Photodiodes that register red light are typically the most sensitive of the visible bands in the near infrared region so red sensors will be registering both red light and a high level of near infrared once the near infrared sensor is removed (Verhoeven et al. 2009). The blue band, which is the band being used for near infrared in the modified X3, will not absorb as large a portion of near infrared light (Verhoeven et al. 2009). This would result in higher values being registered for red light by the modified X3 and thus a negative NDVI value because it effectively changes the formula for the modified X3 camera. The formula will change because the red band is really registering red plus NIR, while the blue band is only registering NIR. The resulting formula is then:

$$NDVI = \frac{\rho_{nir} - (\rho_{red} + \rho_{nir})}{\rho_{nir} + (\rho_{red} + \rho_{nir})} \rightarrow NDVI = \frac{-\rho_{red}}{2\rho_{nir}}$$

Spatial Variation

The patterns observed once the index maps had been separated into quantiles were significantly different between the two sensors (Table 2 and Figures 11, 12, 13, and 14). Upon visual inspection of the index maps, either before or after transformation to the ordinal rating scale, the two maps do not appear similar and the same trends in vegetation are not present. Vignetting effects would likely have an impact on this as NDVI values were lower in areas where vignetting was most apparent. Vignetting was also only present in NDVI maps from the modified camera, resulting in large differences in values in some locations, which likely had a sizable impact on detecting spatial patterns.

Image Format

Capturing images and storing them in jpeg format is important to address, as this is the format that images from the modified X3 camera were stored in. It is well established in the literature that capturing images in jpeg format is not recommended when radiometric fidelity is desired, and that storing of images in RAW format is preferable (Verhoeven 2009). RAW format refers to image storage where DNs are not compressed prior to storage to preserve all characteristics of the image (Verhoeven et al. 2009). Klaas (2016) found that observed differences between modified and multispectral derived NDVI were due to spectral contamination due to overlapping bands rather than the loss of spectral artefacts. Additionally, Lebourgeois et al. (2008) reported that using unprocessed images did not improve results of image analysis; and capturing RAW images didn't change the correlation between spectral bands and surface characteristics. While jpeg compression is likely to impact the ability to derive detailed quantitative information from the sensor, it does not explain the low relative values obtained for the near infrared band and resultant negative NDVI values produced by the modified X3.

Conclusions

In conclusion, this study showed that there were significant differences between NDVI maps produced by the modified DJI Zenmuse X3 RGB camera and the MicaSense RedEdge® multispectral camera. The MicaSense RedEdge® appears to be a more accurate means of producing NDVI when compared to the modified X3 camera because it identified logical changes in chlorophyll throughout grass maturation that was observed between sampling dates. As the reflectance of red light increased with senescence, NDVI values are expected to decline, as they did for the RedEdge®. While I have speculated about the cause of the low values for near infrared light collected from the modified X3, to really determine the cause of this difference, a spectral response curve should be generated from the modified X3 using the process outlined in Verhoeven et al. (2009). This would allow the sensitivities of the camera bands to different wavelengths of light to be known, and thus would potentially provide a more complete explanation of the observed differences.

The modified DJI Zenmuse X3 RGB camera does not appear to produce equivalent NDVI maps to those produced by the MicaSense RedEdge®. The RedEdge® recognized expected patterns in grass maturation correctly, as well as produced values characteristic of green vegetation, while the modified X3 camera did not. The vegetation sensing capabilities of the modified DJI X3 camera does not appear to be equivalent to that of the MicaSense RedEdge® multispectral camera with respect to the NDVI produced; and therefore I reject my null hypothesis that the modified DJI X3 RGB camera is capable of producing equivalent NDVI index maps to those produced from the MicaSense RedEdge® multispectral camera, as well as the null hypothesis that the two cameras will recognize the same patterns in spatial variation in vegetation.

Literature Cited

- Aerial Media Pros. 2015. AerialAgPros.com - Aerial scouting, mapping, and precision ag drones | how to: NDVI processing. [internet]. [cited 2017 Mar 27]; Available from: <http://www.aerialagpros.com/blank>
- Candiago S, Remondino F, De Giglio M, Dubbini M, Gattelli M. 2015. Evaluating multispectral images and vegetation indices for precision farming applications from UAV images. *Remote Sensing*, **7**:4026–4047
- Cordon G, Lagorio MG, Paruelo JM. 2016. Chlorophyll fluorescence, photochemical reflective index and normalized difference vegetative index during plant senescence. *Journal of Plant Physiology*, **199**:100–110
- Darmont A. 2009. Spectral response of silicon image sensors. [internet]. [cited 2017 Apr 2]; Available from: <http://www.aphesa.com/documents.php?class=wp>
- DJI. 2017. Zenmuse X Series cameras comparison - DJI. [internet]. [cited 2017 Apr 17]; Available from: <http://www.dji.com/products/compare-xcamera>
- ESRI. 2016. ArcMap Desktop.
- Herring JW and D. 2000. Measuring vegetation (NDVI & EVI). [internet]. [cited 2017 Mar 26]; Available from: https://earthobservatory.nasa.gov/Features/MeasuringVegetation/measuring_vegetation_2.php
- IBM Corp. 2016. IBM SPSS Statistics for Windows.
- Klaas P. 2016. Towards calibrated vegetation indices from UAS-derived orthomosaics. *Proceedings of the 13th International Conference on Precision Agriculture*. [internet]. [cited 2017 Apr 2]; Available from: https://www.researchgate.net/profile/Klaas_Paul/publication/306503112_Towards_Calibrated_Vegetation_Indices_from_UAS-derived_Orthomosaics/links/57beb27d08aeb95224d09cf2.pdf
- Lebourgeois V, Bégué A, Labbé S, Mallavan B, Prévot L, Roux B. 2008. Can commercial digital cameras be used as multispectral sensors? A crop monitoring test. *Sensors*, **8**:7300–7322
- Matese A, Toscano P, Di Gennaro S, Genesio L, Vaccari F, Primicerio J, Belli C, Zaldei A, Bianconi R, Gioli B. 2015. Intercomparison of UAV, aircraft and satellite remote sensing platforms for precision viticulture. *Remote Sensing*, **7**:2971–2990

- Van der Meij B. 2016. Measuring the legacy of plants and plant traits using UAV-based optical sensors. Geographical information management and applications thesis, Utrecht University, Utrecht, Netherlands. [internet]. [cited 2017 Apr 16]; Available from: https://dspace.library.uu.nl/bitstream/handle/1874/337073/MasterThesis_GIM_A_BvdMeij.pdf?sequence=1
- MicaSense. 2016. RedEdge — MicaSense. [internet]. [cited 2017 Mar 27]. <https://www.micasense.com/rededge>
- Monteith JL. 1972. Solar radiation and productivity in tropical ecosystems. *Journal of Applied Ecology*, **9**:747
- Nebiker S, Lack N, Abächerli M, Läderach S. 2016. Light-weight multispectral UAV sensors and their capabilities for predicting grain yield and detecting plant disease. *The International Archives of the Photogrammetry, Remote Sensing and Spatial Information Sciences*. p. 963–970. [internet]. [cited 2017 Apr 9]; Available from: <http://www.int-arch-photogramm-remote-sens-spatial-inf-sci.net/XLI-B1/963/2016/isprs-archives-XLI-B1-963-2016.pdf>
- Nex F, Remondino F. 2014. UAV for 3D mapping applications: a review. *Applied Geomatics* **6**:1–15
- Pavlović D, Nikolić B, Đurović S, Waisi H, Anđelković A, Marisavljević D. 2014. Chlorophyll as a measure of plant health: Agroecological aspects. *Pesticides and Phytomedicine*. **29**:21–34
- Pix4D. 2017a. Pix4D - Drone mapping software for desktop + Cloud + Mobile. [internet]. [cited 2017 Apr 17]; Available from: <https://pix4d.com/>
- Pix4D. 2017b. Quality report help – support. [internet]. [cited 2017 Apr 5]; Available from: <https://support.pix4d.com/hc/en-us/articles/202558689-Quality-Report-Help#gsc.tab=0>
- Pix4D Support. 2016. Vignetting and dark current correction. – support. [internet]. [cited 2017 Apr 9]; Available from: <https://support.pix4d.com/hc/en-us/community/posts/115000053643-Vignetting-and-Dark-Current-Correction-#gsc.tab=0>
- R Core Team. 2016. R: a language and environment for statistical computing. Vienna: R Foundation for Statistical Computing.

Taylor C. 2015. Radiometric calibration of a modified DSLR for NDVI. Senior thesis, Rochester Institute of Technology, Rochester, New York, United States. [internet]. [cited 2017 Mar 28]; Available from:
<https://www.cis.rit.edu/~cnspci/references/theses/senior/taylor2015.pdf>

Verhoeven GJ. 2009. It ' s all about the format – unleashing the power of RAW aerial photography. *International Journal of Remote Sensing*, **31**:2009–2042

Verhoeven GJ, Smet PF, Poelman D, Vermeulen F. 2009. Spectral characterization of a digital still camera's NIR modification to enhance archaeological observation. *IEEE Transactions on Geoscience and Remote Sensing*, **47**:3456–3468

Appendix A

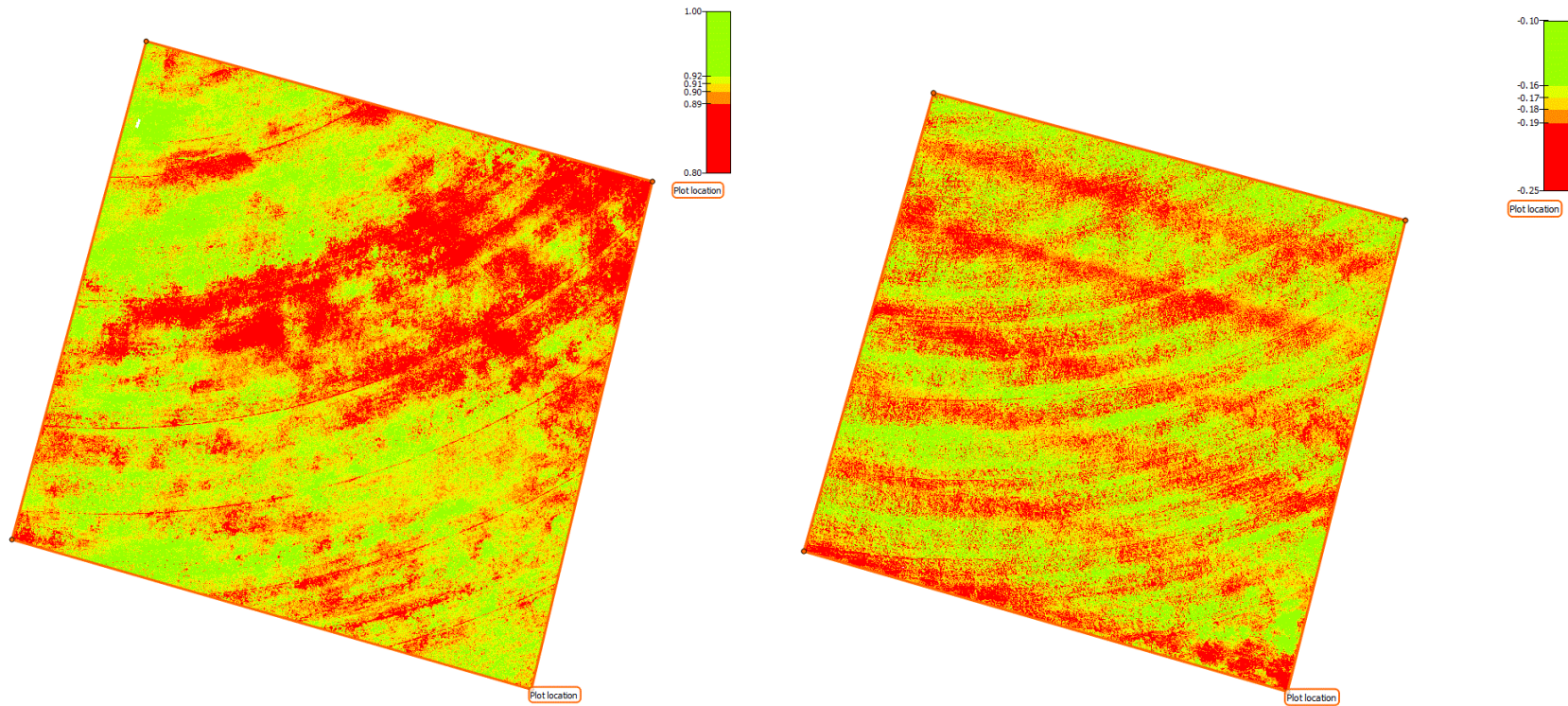


Figure 7: NDVI orthomosaics from the MicaSense RedEdge® (left) and the modified DJI X3 (right) for July 11th, 2016

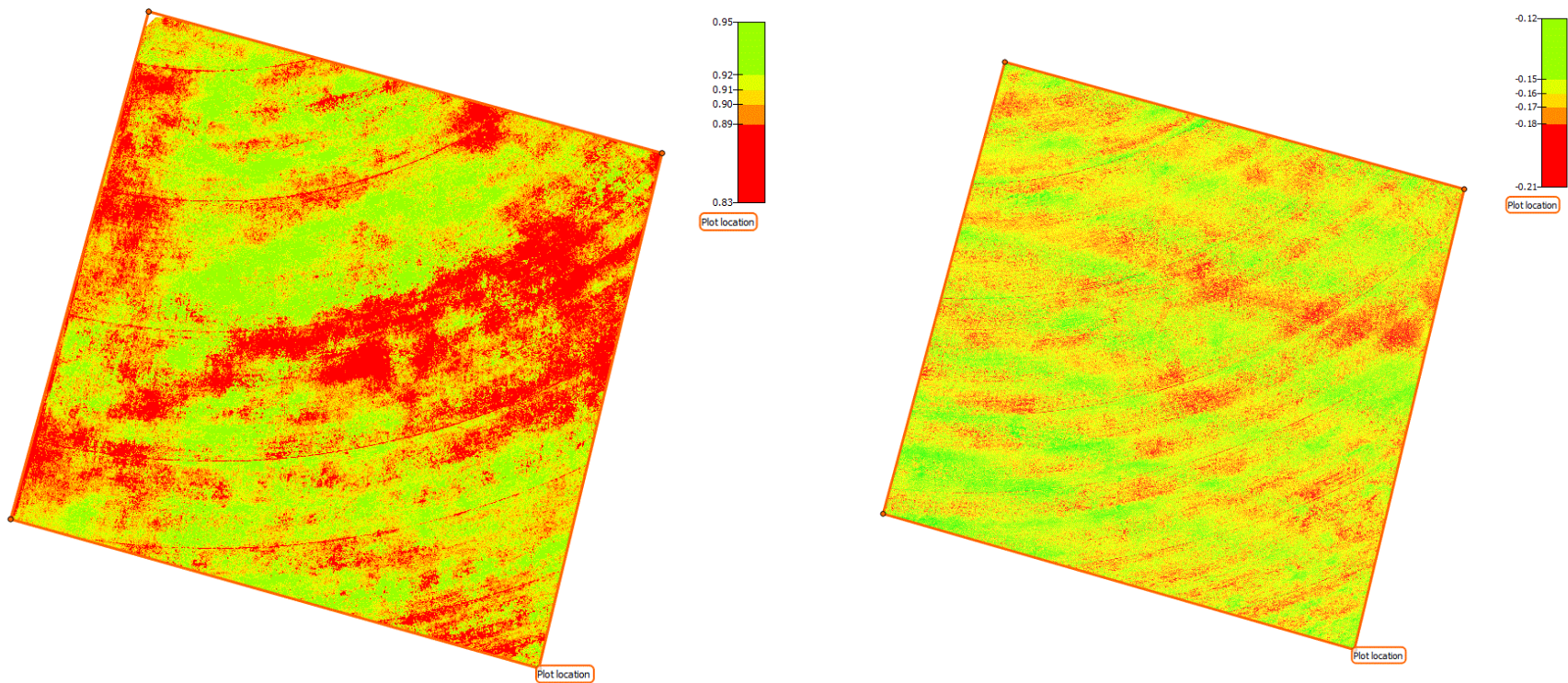


Figure 8: NDVI orthomosaics from the MicaSense RedEdge® (left) and the modified DJI X3 (right) for July 13th, 2016

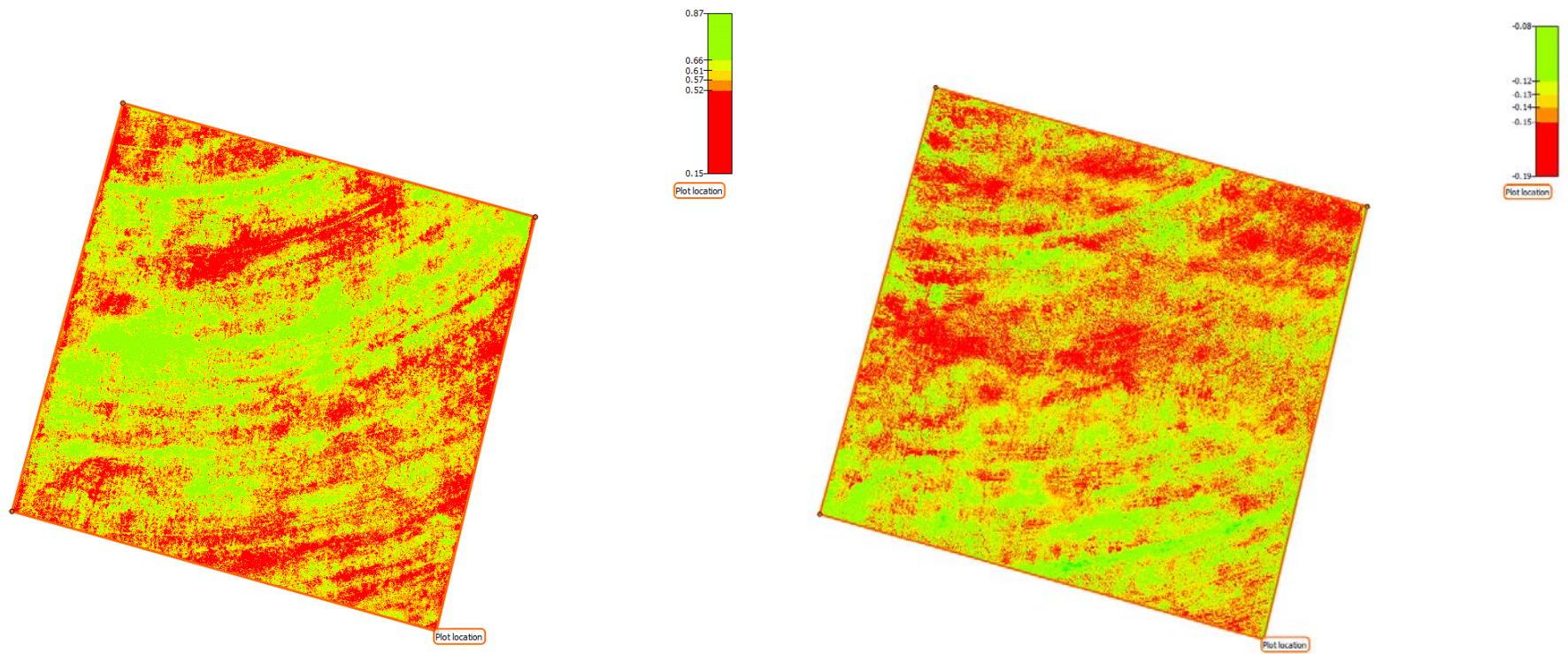


Figure 9: NDVI orthomosaics from the MicaSense RedEdge® (left) and the modified DJI X3 (right) for August 19th, 2016

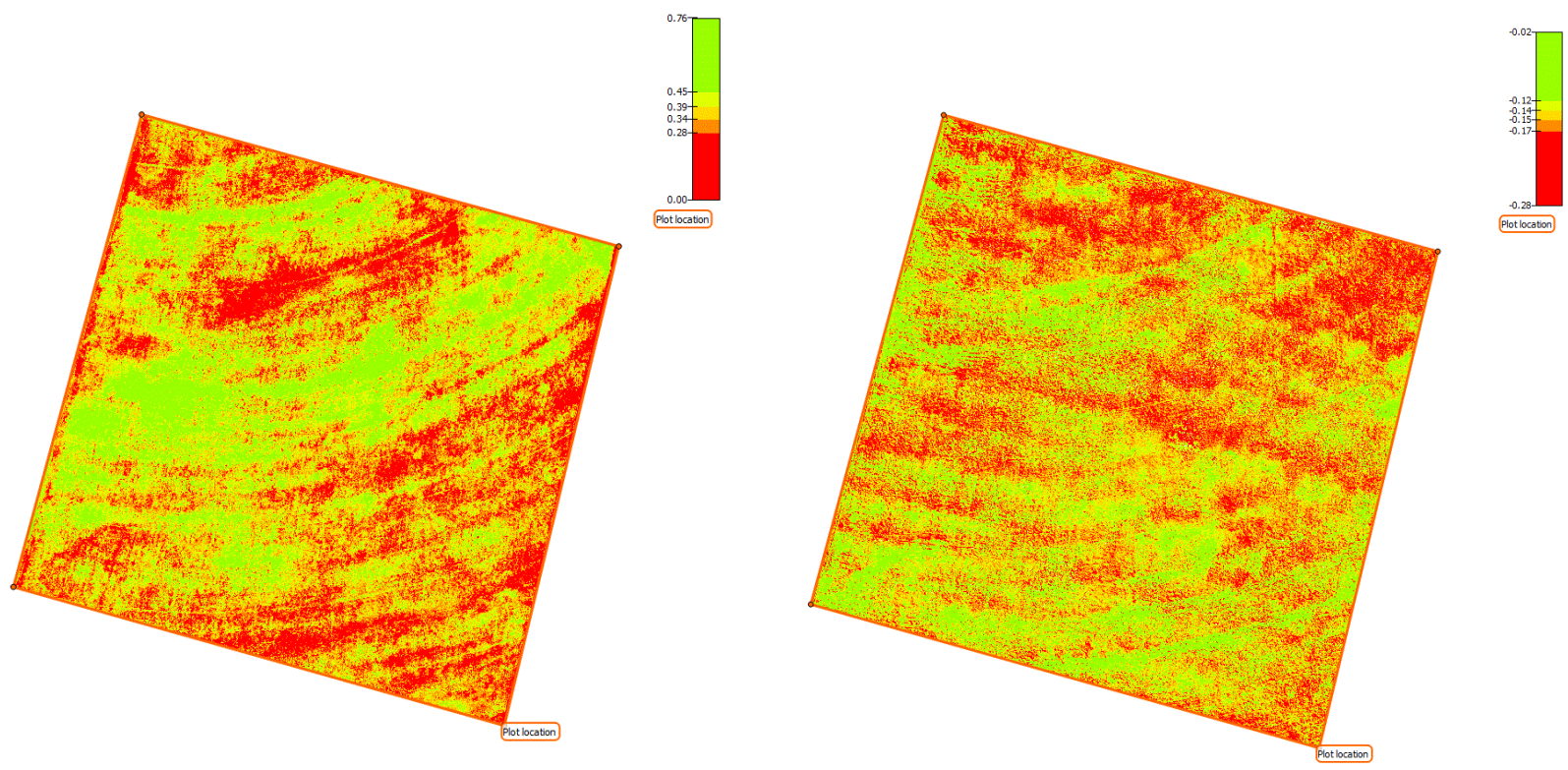


Figure 10: NDVI orthomosaics from the MicaSense RedEdge® (left) and the modified DJI X3 (right) for August 23rd, 2016

Appendix B

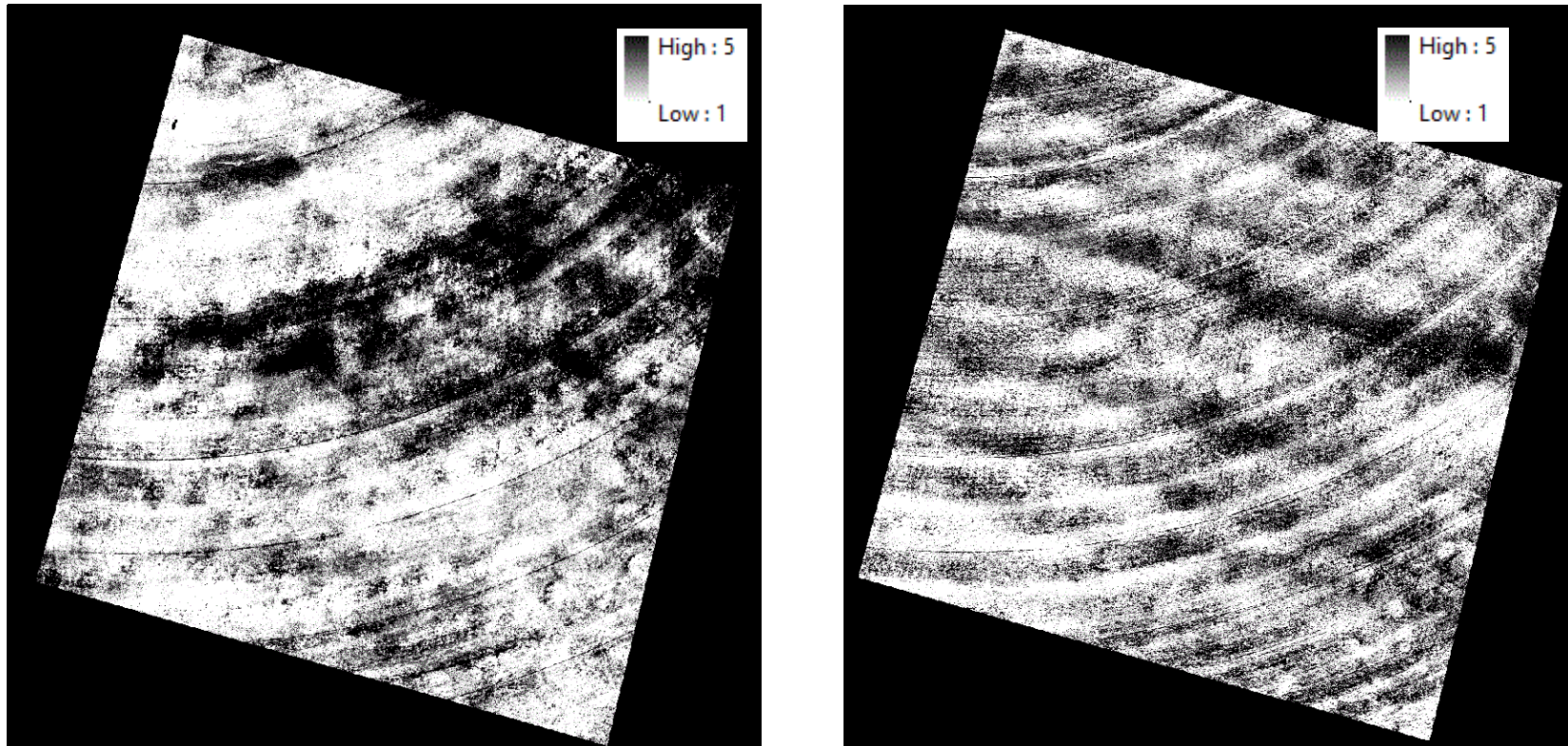


Figure 11: NDVI maps once they had been separated in 20% quantiles for the July 11th, 2016 sampling date from the MicaSense RedEdge[®] (left) and the modified DJI X3 (right).

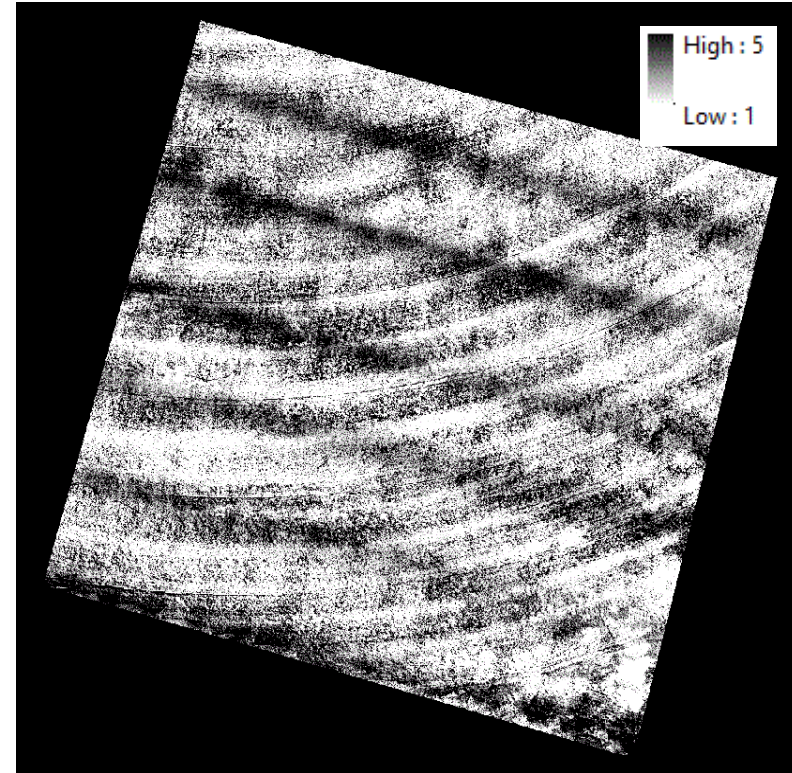
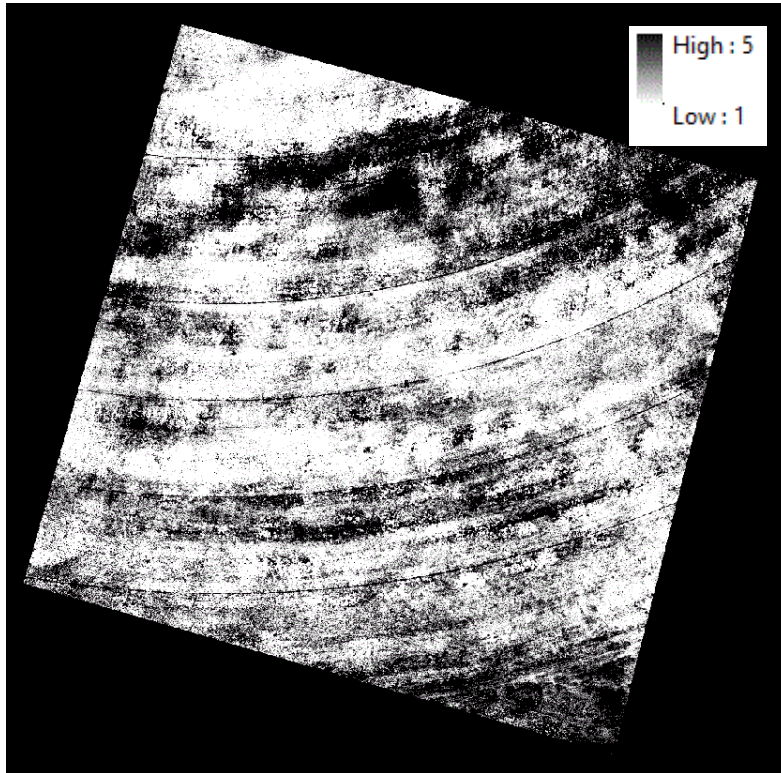


Figure 12: NDVI maps once they had been separated in 20% quantiles for the July 13th, 2016 sampling date from the MicaSense RedEdge[®] (left) and the modified DJI X3 (right).

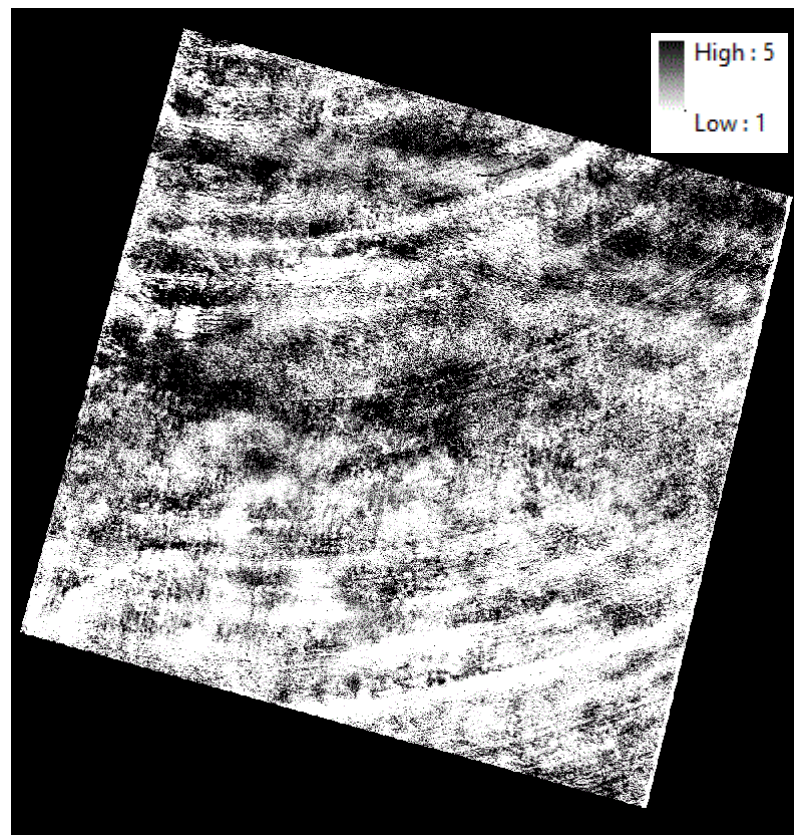
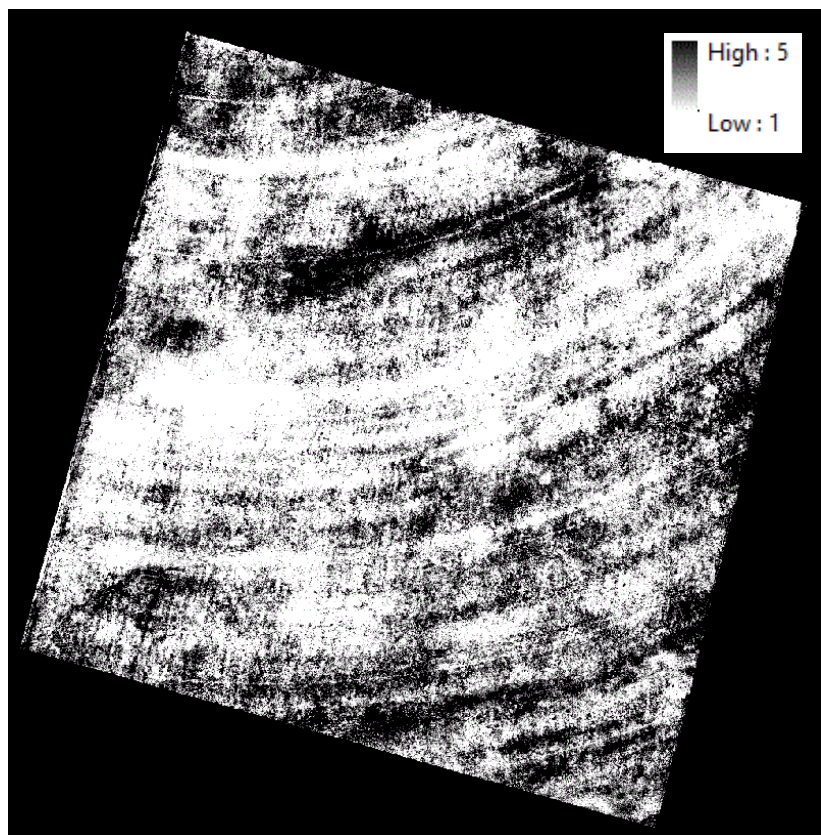


Figure 13: NDVI maps once they had been separated in 20% quantiles for the August 19th, 2016 sampling date from the MicaSense RedEdge[®] (left) and the modified DJI X3 (right).

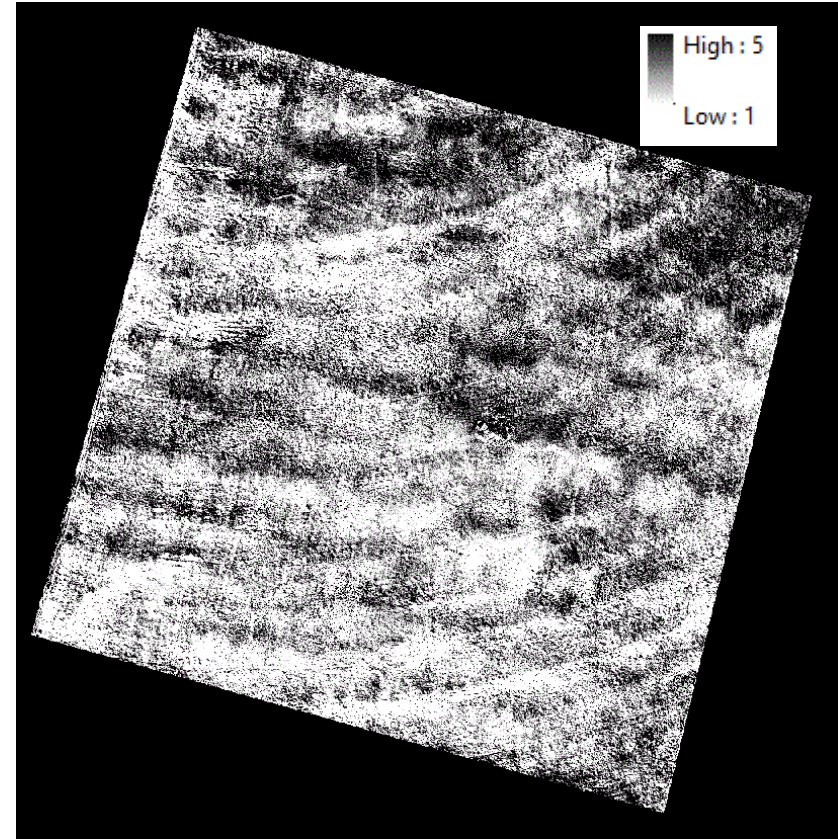
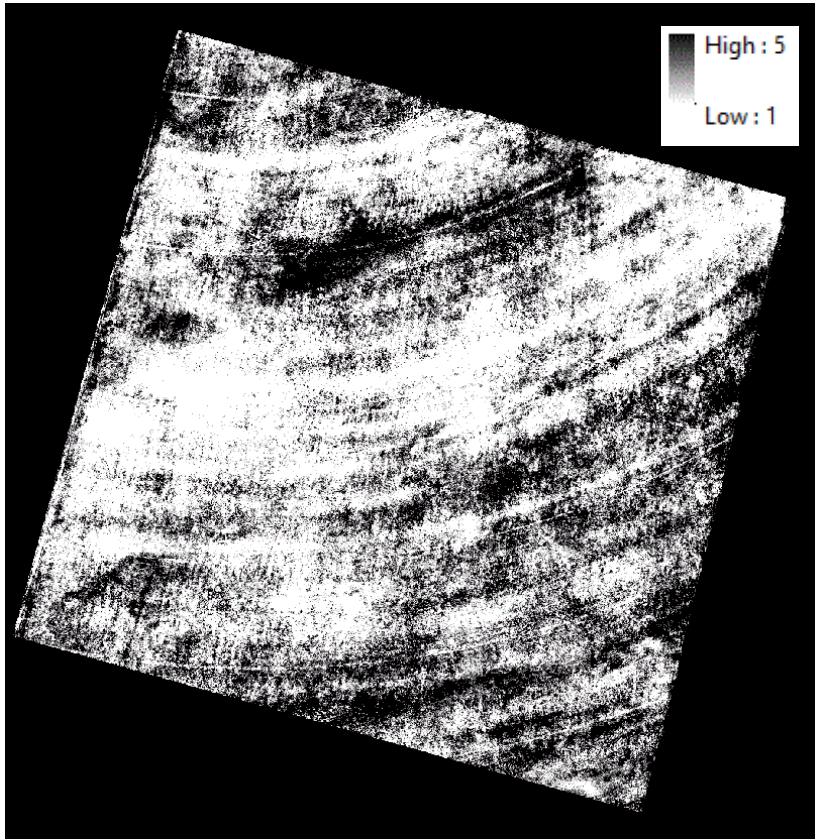


Figure 14: NDVI maps once they had been separated in 20% quantiles for the August 23rd, 2016 sampling date from the MicaSense RedEdge® (left) and the modified DJI X3 (right).

Appendix C

Table 2: Results of the Wilcoxon Signed Ranks test showing the standardized test statistic and the significance of the test.

Date	Standardized Test Stat	Significance
July 11 th	18.586	P<0.0001
July 13 th	1.752	0.08
August 19 th	19.725	P<0.0001
August 23 rd	-6.824	P<0.0001

Appendix D



Figure 15: The DJI Zenmuse X3. This camera has a single lens and one 12 mega-pixel sensor with a Bayer filter array.



Figure 16: The MicaSense RedEdge® multispectral camera. This camera has 5 lenses, one for each spectral band, and 5, 1.2 mega-pixel sensor chips with a separate filter for each chip.